Influence of growing conditions on the reactivity of Ni supported graphene towards CO

E. Celasco, G. Carraro, M. Smerieri, L. Savio, M. Rocca, and L. Vattuone

Citation: The Journal of Chemical Physics **146**, 104704 (2017); doi: 10.1063/1.4978234
View online: http://dx.doi.org/10.1063/1.4978234
View Table of Contents: http://aip.scitation.org/toc/jcp/146/10
Published by the American Institute of Physics

Influence of growing conditions on the reactivity of Ni supported graphene towards CO

E. Celasco,[1,2,a)] G. Carraro,[1,2] M. Smerieri,[1] L. Savio,[1] M. Rocca,[1,2] and L. Vattuone[1,2]
[1]*Dipartimento di Fisica, Università di Genova, 16146 Genova, Italy*
[2]*IMEM-CNR Unità Operativa di Genova, 16146 Genova, Italy*

(Received 27 October 2016; accepted 23 February 2017; published online 14 March 2017)

Free standing graphene is chemically inert but, as recently demonstrated, CO chemisorption occurs at low crystal temperature on the single layer grown by ethene dehydrogenation on Ni(111). Such layer is inhomogeneous since different phases coexist, the relative abundance of which depends on the growth conditions. Here we show by X ray photoemission and high resolution electron energy loss spectroscopies that the attained CO coverage depends strongly on the relative weight of the different phases as well as on the concentration of carbon in the Ni subsurface region. Our data show that the chemical reactivity is hampered by the carbon content in the substrate. The correlation between the amount of adsorbed CO and the weight of the different graphene phases indicates that the top-fcc configuration is the most reactive. *Published by AIP Publishing.* [http://dx.doi.org/10.1063/1.4978234]

INTRODUCTION

Even if graphene (G) is chemically inert, chemisorption on it has been recently reported under special conditions. For example, it has been shown that G can react with atomic H[1] and that its reactivity is affected by mechanical strain. G supported on silicon carbide reacts with aryl radicals generated *in situ* from diazonium,[2] while G on Ni(111) promotes the dehalogenation reaction of 1,3,5-tris(4-bromophenyl)benzene.[3] It is also known that covalent functionalization takes place more effectively in presence of large electron hole charge fluctuations, as observed for G supported on SiO_2 and Al_2O_3.[4] The interest in the topic is witnessed by the recent publication of reviews on G functionalization methods,[1,5] which also provides a more complete set of examples.

For less reactive environments/adsorbates, adsorption enthalpies in the range appropriate for physisorption have been reported at regular graphene sites.[6] Albeit usually weaker, physisorption can compete with chemisorption for sufficiently large molecules. The physisorption enthalpy can be modulated by doping the layer. Intercalation of different species such as Eu or Cs may induce strong n-doping[7] and enhance the physisorption energy, as in the case of naphthalene molecules on Eu-intercalated G. On the contrary, p-doping causes a weakening of the physisorption interaction.[8]

In a recent investigation, we have demonstrated that weak CO chemisorption occurs at pristine G/Ni(111) sites[9,10] while a G layer grown on polycrystalline Cu is unreactive under identical conditions.[11] The value of the desorption energy of CO/G/Ni(111) as well as its reversible nature indicates the occurrence of non-dissociative chemisorption at pristine sites up to a coverage as high as 0.33 monolayers (MLs). This unexpected result indicates that the nature of the substrate and the strength of its interaction with G are critical in determining the chemical properties of the G layer on its vacuum side. Theoretical calculations trying to explain this result also appeared recently.[12]

The importance of the substrate was suggested also for the above-mentioned de-halogenation reaction of halogenated compounds[3] since the barrier for the cleavage of the C-Br bond is 1.4 eV larger on free standing graphene than for G/Ni(111).

In the present paper, we go forward in this analysis and investigate the dependence of the reactivity of the G/Ni(111) system on the particular phase formed. It is indeed well known that the G/Ni(111) layer is not uniform, but C atoms occupy different sites, forming domains with either top-fcc, top–bridge, or the less stable top-hcp geometry. Such configurations are characterised by different distances from the substrate and different bond strengths and their relative abundance depends on the growth parameters.[13,14] In addition, at high temperature, rotated G domains may form. Finally, on Ni(111), the alternative mechanisms of nickel carbide formation and carbon dissolution into the bulk may compete with G growth in a way which depends on both pre-growth treatments and growth temperature.[15] By a combination of high resolution electron energy loss spectroscopy (HREELS) and X-ray photoemission spectroscopy (XPS) experiments, we relate the CO adsorption yield to the protocol used to grow the G layer and to the fractional coverage of the different phases, concluding that the top-fcc configuration is the most reactive one. This conclusion is supported also by the reanalysis of our STM data reported in the supplementary material.

EXPERIMENTAL

Experiments have been performed in an ultra-high vacuum (UHV) chamber with base pressure $P \sim 2 \times 10^{-10}$ mbar, equipped with a HREEL spectrometer (Delta 0.5 by SPECS) and with a non-monochromatized X-ray source and hemispherical analyser (DAR 400 and EA125 by Omicron). The apparatus also hosts typical facilities for sample cleaning and

a)Author to whom correspondence should be addressed. Electronic mail: celasco@fisica.unige.it

TABLE I. Growth parameters for the different G/Ni(111) layer preparation protocols.

Growth protocol	Temperature T_g (K)	Ethene dosing pressure (mbar)	Growth time (s)	Ethene dose (l)	Waiting time thermalization without ethane gas (s)
753 K SD	753	5×10^{-6}	660	2500	600
823 K DD1	823	1×10^{-5}	660	5000	600
823 K DD2	823	1×10^{-5}	660	5000	600
873 K DD	873	1×10^{-5}	660	5000	600
Segregation	688	···	1800	···	···

residual gas analysis, a low energy electron diffractometer (LEED) and a four-degrees of freedom manipulator. The sample can be cooled down to a temperature T = 87 K by fluxing liquid nitrogen and heated to T > 1200 K by electron bombardment. The substrate used for the growth of G *in situ* is a commercial Ni(111) single crystal disk of 10 mm diameter, aligned to less than 0.1° from the (111) direction (by Surface Preparation Laboratory).

Before each preparation, the Ni(111) crystal was cleaned by sputtering cycles with 3 keV Ne^+ ions followed by annealing to T = 1200 K. Surface cleanliness and order were checked by XPS and LEED, respectively. In addition, for a more efficient removal of C dissolved in the near-surface region, before graphene growth, we performed several cleaning cycles in which the sample was exposed to ~2.5 L of O_2 at T = 673 K and then annealed to 783 K under UHV conditions. In particular, as described in more detail later, this procedure has been applied before graphene growth with protocol 823 K DD2.

Single layer G films were grown *in situ* by surface catalysed dehydrogenation of ethene, according to well established recipes.[11,15] The substrate growth temperature (T_g) was varied between T_g = 753 K and T_g = 873 K, for the different growth protocols. Ethene was introduced into the UHV chamber through a doser placed ~1 cm away from the Ni(111) surface. Under these conditions, we estimate an increase in the local pressure of approximately a factor of 5 with respect to the value measured in the UHV chamber.[16] The substrate was exposed to ethene for 660 s either at $P = 5 \times 10^{-6}$ mbar (~2500 l, referred to as single dose, SD, in the following) or at $P = 1.0 \times 10^{-5}$ mbar (~5000 l, double dose, DD). The sample was kept eventually at T_g for 10 min after pumping ethene off. Alternatively, G was obtained by segregation of C atoms dissolved in the bulk by annealing the clean Ni(111) crystal to 788 K for 30 min in UHV.

The protocols implemented are summarized in Table I.

CO exposure was performed by backfilling the chamber, after cooling the G/Ni(111) sample to RT or to 87 K. The composition of the carbon films was evaluated by XPS, while CO adsorption was monitored by HREELS. The XPS spectra were recorded at normal emission, using $Al_{K\alpha}$ excitation photon. The binding energy, E_b, has been calibrated on the metallic Ni $2p_{3/2}$ line which, in absence of dissolved carbon, is located at 852.6 eV.[17,18] Detailed analysis of the C 1s region was performed by fitting the photoemission signal with different contributions (see Figure 3(b)) described by using Doniach Sunjic functions. HREEL spectra were recorded in-specular, with a primary electron energy E_e = 4.0 eV and an angle of incidence of the electron beam $\theta_i = 62°$ with respect to the surface normal. The typical energy resolution is ~4.0 meV. In order to allow for a reliable comparison of the different spectra, the measured intensity (I_{meas}) is normalized with respect to the average intensity of the inelastic tail in the flat region between 400 meV and 500 meV ($\langle I_{[400;500]\ meV} \rangle$). The plotted intensity (I_{norm}) results then from the normalization,

$$I_{norm} = \frac{I_{meas}}{\langle I_{[400;500]\ meV} \rangle}.$$

Finally, the traces were vertically shifted for sake of clarity, whenever appropriate.

RESULTS

As mentioned in the Introduction, different adsorption configurations exist for graphene on Ni(111), see schematic picture in Fig. 1. Combined high resolution XPS experiments and Density Functional Theory (DFT)[13] calculations indicate that, in the most stable geometry, the two C atoms of the G unit cell occupy top and fcc sites of the underlying Ni(111) lattice; this configuration is referred to as top-fcc in the following. A nearly iso-energetic assembly corresponds to C atoms in top and bridge sites (top-bridge),[13] while the condition in which C atoms sit in top and hcp sites (top-hcp) is slightly less stable. The relative concentration of these configurations depends drastically from the growing parameter conditions.[13]

The different arrangements are characterized by different C 1s line shapes, which can be distinguished easily

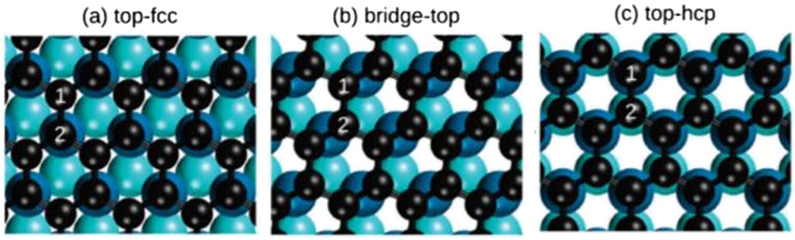

FIG. 1. Schematic different configurations of graphene: top-fcc (a), bridge-top (b), and top-hcp (c). Reprinted with permission from Zhao *et al.*, J. Chem. Phys. Lett. **2**, 759–764 (2011). Copyright 2011 American Chemical Society. Color legend: black C, blue Ni first layer, light blue Ni second layer.

in high resolution XPS experiments performed with synchrotron radiation. Indeed, graphene in top-fcc geometry[19] is characterized by a doublet in the C 1s region at 285.1 eV and 284.5 eV; the top-bridge and top-hcp domains, on the contrary, present XPS spectra with a single component centered at 284.8 eV and 285.3 eV, respectively.[13] Though it is not possible to resolve such contributions with a conventional laboratory X-ray source, their relative weight modifies the shape of the photoemission peak and the position of its maximum, so that useful information can be extracted by fitting the C 1s peak with the components determined in the synchrotron radiation experiments in literature.[13] A careful calibration of the energy scale is necessary for this scope and was obtained by using the Ni(2p) peak of metallic Ni (free from dissolved C) as a reference.20

The core-level shifts (CLSs) of the two non-equivalent C atoms (C1 and C2) with respect to free standing graphene have been estimated theoretically.[13] The values for the configurations relevant to the present paper are summarized in Table II for the sake of clarity.

In order to understand how growth conditions may influence the reactivity of the G/Ni(111) film with respect to CO adsorption, we have grown the G layers under the different conditions summarized in Table I. The samples were eventually cooled down to 87 K and exposed to 40 l of CO. Figure 2 shows the outcome of HREELS inspection for the different growth protocols.

Stable CO adsorption occurs on all the samples, as witnessed by the presence of a CO stretch vibration around 256 meV (this EEL peak is absent when the same samples are exposed to CO at room temperature[9]). As witnessed by the intensity of the energy loss, the attained coverage after the dose is different for the different growth protocols; in particular, it is largest for the films produced at T_g = 823 K and significantly lower for the other cases. However, two nominally identical preparations (addressed as 823-DD1 and 823-DD2) exhibit remarkably different reactivity towards CO.

The peak around 90 meV, present in all the spectra, corresponds to the H_2O libration mode and is indicative of some little water contamination; most likely, due to unwanted adsorption from the residual gas. Since the intensity of such energy loss is not correlated with the amount of adsorbed CO, we conclude that water acts as a spectator, and we shall not discuss it further.

We underline that no CO adsorption is detected when the exposure is performed at RT (see Ref. 9). Besides providing the information that the G layer is inert at 300 K, this result witnesses also the growth of a continuous G film fully covering

TABLE II. Theoretically estimated core level shifts for the two inequivalent carbon atoms for the different configurations of G on Ni(111) addressed in this paper. Data taken from Ref. 13.

Configuration	Core level shift of C1 (eV)	Core level shift of C2 (eV)
Bridge-top	−0.40	−0.36
Top-fcc	−0.63	−0.19
Top-hcp	+0.30	+0.31

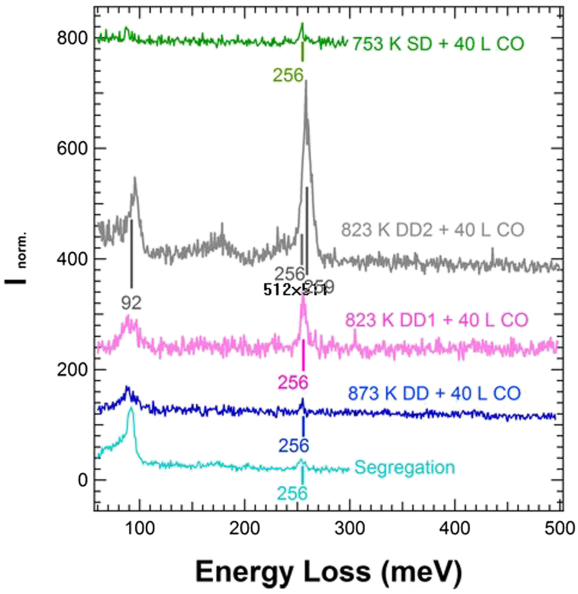

FIG. 2. HREEL spectra recorded after exposing G/Ni(111) layers prepared following the different protocols and cooled at 87 K to 40 l of CO.

the surface. In fact, the presence of bare Ni patches would result in CO adsorption at RT since:

(a) For coverage lower than 0.4 Ml, CO desorption off Ni(111) occurs between 412 and 450 K[21,22] so that it should be observable by HREELS after exposure at RT.
(b) HREEL spectra for CO on Ni(111) exhibit one feature at 236 meV for exposure at 150 K and a doublet at 233 and 250 meV for exposure at RT, the feature at 233 meV being the most intense.[23] No loss at around 230 meV is observed in the present experiment.

In order to understand the reasons of the differences in reactivity observed for our films, we analyzed the X-ray photoemission spectra for each of them recorded before CO exposure. XPS spectra were recorded at RT to prevent uncontrolled CO adsorption from the background pressure. The raw data are reported in Figure 3(a). The spectra of the C 1s region corresponding to the different preparations show a single peak centered at 284.6 eV. They present small differences in shape and intensity, which are associated to the different relative amount of G in top-bridge, top-fcc, and top-hcp configuration, as well as to the amount of nickel carbide (Ni_2C) present at the surface.

By cross-comparison of the XPS spectra with the theoretically estimated core-level shifts reported in Table II it is apparent that:

(a) A significant fraction of domains with top-fcc configuration determines a shift toward lower BE (with respect to free standing graphene) of the centroid of the C 1s feature, since the top-fcc configuration has a contribution with a core level shift (CLS) of −0.63 eV and the average CLS of the two components is −0.41 eV;
(b) A significant fraction of domains with top-bridge configuration causes a (smaller) shift toward lower BE of the centroid because the average CLS is −0.38 eV;

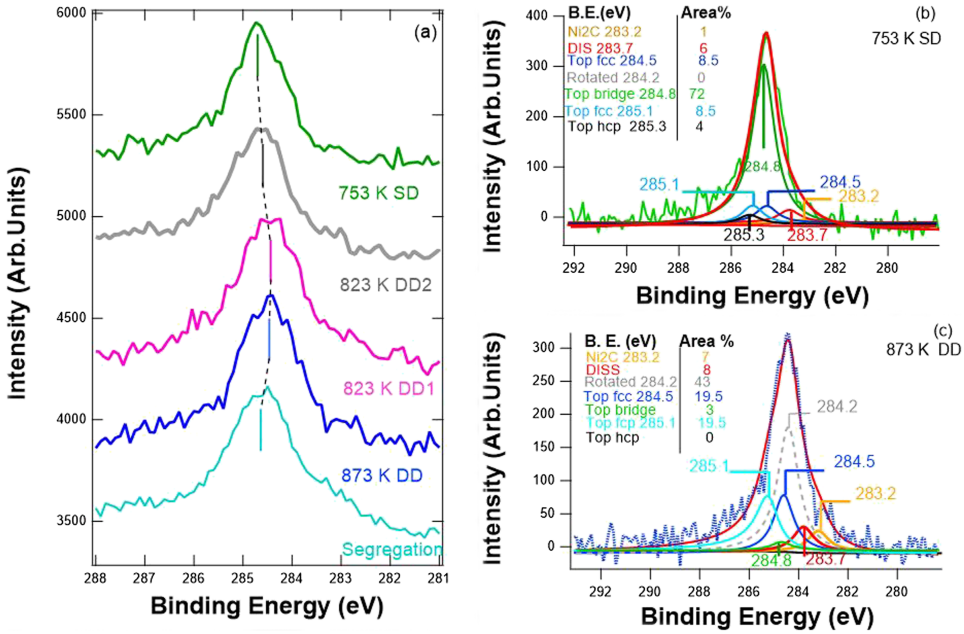

FIG. 3. XPS spectra of C 1s region of all preparations (panel (a)). Example of the result of the XPS fitting procedure shown for SD and DD preparations at 753 K and 873 K (panels (b) and (c), respectively): Top-hcp component (black), top-fcc (blue and light blue), top-bridge (green), rotated graphene (gray), dissolved (red), and Ni_2C (orange).

(c) Domains with top-hcp configuration cause the presence of extra-intensity (i.e., a shoulder) at higher BE since the average CLS of this component is +0.31 eV;
(d) A significant amount of Ni_2C and of dissolved carbon determines extra intensity at lower BE;
(e) A larger width of the C 1s suggests the presence of significant fraction top-fcc domains which are characterized by the largest difference in the CLS of the two inequivalent carbon atoms.

Such qualitative arguments allow us to expect a relatively larger fraction of top-fcc domains to be present for the 823 K D1 ad 873 K DD protocols, which exhibit the largest negative shift of the centroid, and a relatively lower amount for the 753 K and for the segregation protocols, which are characterized by a centroid at higher BE. The comparison of the extra intensity present on the lower binding energy side also provides evidence for the presence of a larger amount of dissolved C (and/or of Ni_2C domains) for the segregation protocol. Detailed one to one comparisons of several different protocols are reported in the supplementary material.

A more quantitative assessment can be obtained by properly fitting the XPS spectra.[24] As we shall see the conclusions obtained from the fit agree with the qualitative considerations presented above.

After removal of a Shirley background, the experimental curves are fitted as the superposition of several components (see Figures 3(b) and 3(c)): a doublet at 285.1 eV and 284.5 eV, corresponding to graphene in top-fcc sites (light blue and blue traces), a singlet at 284.8 eV (top-bridge G, green curve) rotated graphene (284.2 eV), and one at 285.3 eV (top-hcp G, black trace). The slight difference with respect to the values given in literature is required to ensure the convergence of the fit.

We note that two different processes contribute to the growth of G on Ni(111), their relative importance being determined by the temperature of the sample and by the amount of dissolved carbon present in the bulk.[15] The former growth mode is operative at the highest temperature and directly yields graphene from ethene decomposition. The latter process proceeds via the formation of nickel carbide (Ni_2C). Segregation of C may also play a role if a significant amount of C is dissolved in the bulk of the sample.[14,19] For these reasons, we introduced in the fitting procedure two additional components at 283.3 eV (orange curve) and at 283.7 eV (red curve), corresponding to Ni_2C and dissolved C, respectively.[15,20]

The outcome of the fitting procedure over all the investigated samples is summarized in the histograms of Figure 4. Panel (a) shows the total amount of carbon, obtained by taking into account the total area of the C 1s peak. The total XPS intensity is strongly variable, with a maximum difference of ~30% between the smallest and the largest value. Panel (b) reports the different graphenic (top-hcp, top-bridge, and top-fcc) and non-graphenic (Ni_2C and dissolved C) components for each film. For the preparation at 873 K-DD, an additional contribution of rotated graphene (E_b = 284.2 eV,[15] a species which forms especially above Ni_2C) is also considered. Finally, in panel (c), we plot the CO stretch peak intensity detected by HREEL and normalized to the inelastic background measured after 40 l exposure at 87 K.

The following considerations arise,

(1) First of all, we underline that the information retrieved by XPS spectra recorded at RT is representative of the conditions present at 87 K, the temperature used for CO adsorption. Indeed the amount of Ni_2C and of dissolved C is not expected to change below RT since diffusion and conversion of carbide into G are quenched. On the other hand, the relative population of the different G configurations can change with crystal temperature. According to Ref. 13, the top-fcc component is found to increase by less than 15% when decreasing the surface temperature from 300 K to 150 K. Whether the trend persists till 87 K, i.e., at the temperature of our experiments, is not known and cannot be determined with a non-monochromatized X-ray source. Therefore, the relative

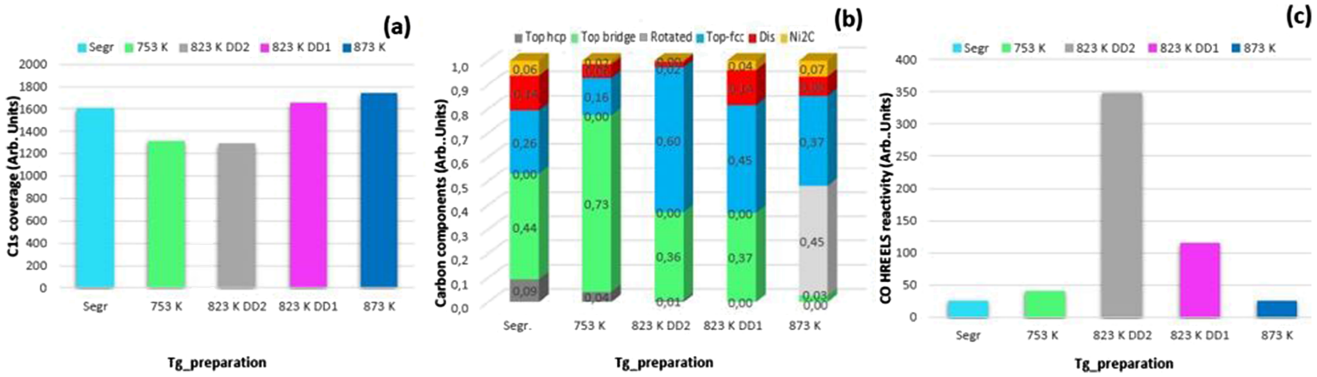

FIG. 4. Histograms summarizing the results of the fitting procedure on the XPS spectra of Figure 3(a). (a) Total amount of C, (b) partitioning of the C 1s intensity into the different graphenic (top-hcp, top-bridge, and top-fcc) and non-graphenic (Ni_2C and dissolved C) components; (c) intensity of the CO stretch peak detected in the HREEL spectra of Figure 2, normalized to the inelastic background, after 40 l exposure at 87 K.

concentration of the different G moieties estimated at RT represents a lower limit for the top-fcc species and an upper limit for the top-bridge one (which must show the opposite behavior in order to conserve the total G coverage).

(2) The spectra with the highest carbon content correspond to those with a significant amount of nickel carbide and/or of dissolved carbon, as estimated considering an escape length of the photoemitted electrons of ~5 nm. This indicates that the surface is covered almost entirely with single layer graphene with a maximum contribution of the bilayer amounting to 15%. The extra estimated 15% of C is due either to Ni_2C or to dissolved C in the bulk. The amount of adsorbed CO present after 40 l dose at 87 K decreases when the amount of non-graphenic carbon increases.

(3) The amount of graphene in top-hcp configuration is very small and decreases with increasing temperature in agreement with DFT calculations, which predict it to be less stable than top-fcc and top-bridge graphene.

(4) The two preparations at 823 K-DD are not equivalent. They correspond to G layers grown either on a Ni substrate obtained following a "standard" cleaning procedure (823 K-DD1, pink trace in Figure 3(a)) or prepared by repeated sputtering and annealing cycles to deplete the near sub-surface Ni layers from dissolved C (823 K-DD2, grey trace). As evident in the chart of Figure 3(b), these two layers are characterized by a quite different amount of Ni_2C, of dissolved C and of top-fcc graphene; in both cases, top-hcp G is missing and top-bridge G is present in similar amounts. The remarkable difference in reactivity indicates that the presence of Ni_2C and/or dissolved C inhibits CO adsorption, and on the other hand that top-bridge G is not the reactive species. This comparison proves, therefore, that top-fcc G is the most reactive phase. Analysis of the composition of the C 1s line for the 753 K-SD and 823 K-DD1 and DD2 samples confirms this statement. Moreover, the 753 K SD preparation has twice as much G in the top bridge configuration than both the 823 K DD1 and 823 K DD2 protocols, in agreement with the lower reactivity of the former layer.

(5) The reactivity of G obtained by the 753 K-SD protocol, despite the lower amount of top-fcc G, is slightly higher than for G obtained by segregation and for the 873 K-DD. Since the preparation at 753 K-SD presents a lower amount of Ni_2C and of dissolved C, this indicates that the reactivity is not only a function of the amount of top-fcc G or non-graphenic carbon alone but it depends on a combination of the two parameters.

Rotated graphene is basically inert, since the reactivity of the 873 K-DD sample, the only one in which rotated G domains are present, is low.

Ni_2C cannot be present at the surface in large amount since we would then observe CO adsorption on it, contrary to experimental outcome. (In our previous publication, we stated wrongly that STM inspection showed bare Ni_2C areas by after CO adsorption.[25] A reanalysis of such data showed that such conclusion was not really supported by the data.) It can therefore be only immediately below rotated graphene domains.

The qualitative considerations summarised above are supported by inspection of the graphs reported in Fig. 5. It is evident that the reactivity is not directly correlated with the amount of top-bridge G (panel (a)) and top-fcc G (panel (b)). On the contrary, it reasonably correlates with the amount of top-fcc/Ni_2C ratio (panel (c)).

Though discriminating between the effect of Ni_2C and of dissolved C is not straightforward, a poisoning effect of the former species seems more reasonable for two reasons. First, dissolved carbon may be diluted in the sample and, if sufficiently deep, it would not be expected to affect the reactivity of the adlayer. Second, due to stoichiometry, a 6% coverage of Ni_2C corresponds to 24% coverage of the substrate area; therefore, it is not unreasonable that the presence of a limited signal due to carbide (which is covered by graphene) influences significantly the overall reactivity.

A closer inspection of the HREEL spectra recorded for the 823 K-DD1 and 823 K-DD2 samples shows a different CO-stretch frequency in the two cases. To better understand the phenomenon, in Figure 6, we compare the spectra recorded after subsequent exposure of these layers to 1 l and 40 l of CO at 87 K. In both cases, the CO-stretch vibration at 256 meV

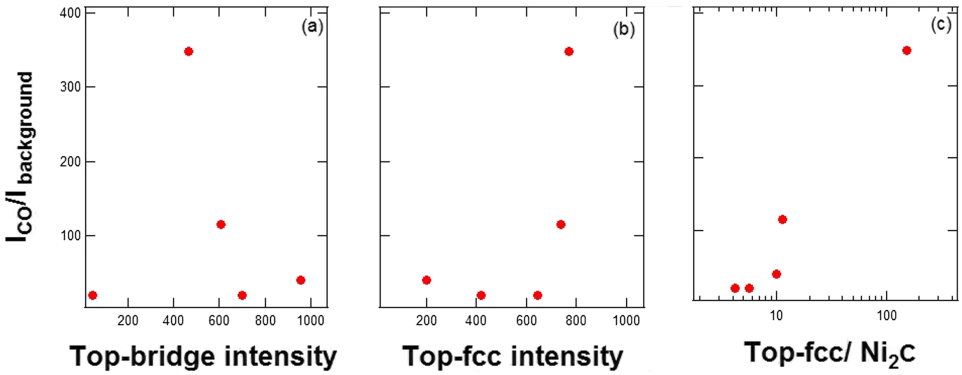

FIG. 5. Intensity of the CO stretch feature (normalised to the inelastic background) vs. intensity, normalited to the backround, of the top-bridge component (circles, (a)), of the top-fcc component (circles (b)), and of the top-fcc/Ni_2C ratio (triangles (c)).

is already evident after 1 l of exposure, its intensity being only slightly larger for the C-depleted sample (823 K-DD2). Increasing the exposure to 40 l CO causes an increase in the intensity of the loss by more than a factor of three for the 823 DD2 sample, leaving the spectrum for the 823 DD1 nearly unaffected. The increase in the intensity of the CO stretch for the C depleted sample is accompanied by a 4 meV blueshift of the CO stretching frequency. These observations indicate that a higher local CO coverage is obtained for T_g = 823 K on the C depleted sample and that such molecules vibrate at a higher frequency due to the stronger dipolar interaction. Possibly the increase in the CO stretch frequency correlates also with a significant decrease in the adsorption energy with increasing coverage.

Our data allow thus to conclude that the reactivity of single layer graphene on Ni(111) with CO is due mostly to its top-fcc component.

In our previous communication,[9] we reported by STM that CO ad-molecules cover the whole graphene layer uniformly. STM inspection did not allow to estimate the relative coverage of top-fcc and top-bridge G, since the number of explored areas was insufficient for a reliable statistical analysis, nor to determine the nature of the graphene below the CO admolecules. However, the reanalysis of these data, presented in the supplementary material, revealed the presence of bare top-hcp areas after CO exposure at 87 K. This result is in agreement with the conclusion about the inertness of top-hcp graphene deduced from the present XPS data analysis.

The reanalysis of the STM images did not confirm the existence of bare Ni_2C patches either. This outcome is in accord with existing literature which agrees that CO attaches on the carbide film grown on Ni(111) already at room temperature.

HREELS inspection proves moreover that CO is monocoordinated with the underlying graphene, i.e., CO sits on top of a C atom. Putting all this information together, we can conclude that the active site coincides with the C atom at the fcc position. Indeed, C atoms at all other possible sites (top, bridge, and hcp) are present for unreactive configurations only. Note that, despite the name, in the top-bridge configuration, the two C atoms per unit cell sit at bridge position with respect to the nickel atoms. The inertness of the top-bridge and of the rotated graphene configurations (when present) agrees with this interpretation. The fcc site is the one for which the C atom is furthest from the underlying Ni. This causes most probably a slight buckling of the top-fcc graphene configuration and the consequent change of the hybridization towards sp^3. If present such buckling must, however, be small since it was not evidenced in DFT calculations nor in the only LEED IV analysis we found in literature.[26]

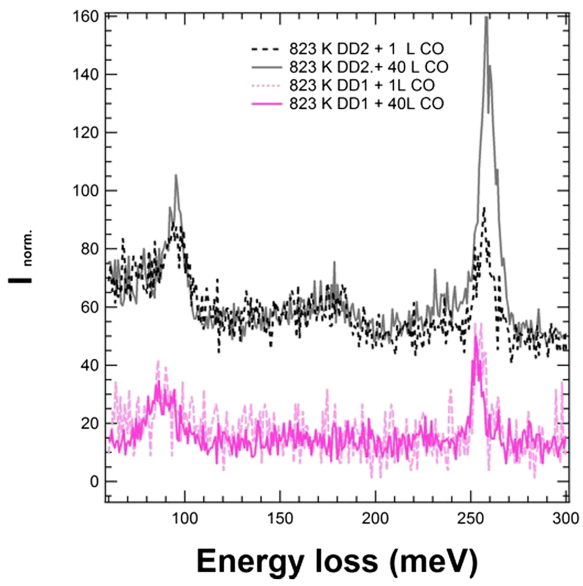

FIG. 6. Comparison of the HREELS spectra recorded after different CO exposures for films grown at 823 K DD on the C-rich (pink spectra) and C-depleted (black spectra) Ni(111) substrate. Dotted traces refer to 1 l of CO exposure, continuous ones to 40 l of CO.

CONCLUSIONS

In conclusion, we have demonstrated experimentally that the reactivity of single layer G on Ni(111) towards CO, a molecule often used as a prototype in surface science, depends on the relative position of the graphene domain with respect to the underlying substrate[20,27] and on the amount of non-graphenic carbon present in the surface layer. Our data allow to determine the reactive site on the graphene layer. Indeed, only in the reactive layer, one graphene C atom sits in the fcc site, while in all other cases either top or bridge or hcp sites are occupied. The reactivity arises therefore from the longer adsorption distance of the fcc C atom from the underlying Ni atom, which sits in the second crystal layer below it. The presence of non-graphenic carbon, either in nickel carbide patches or dissolved in the outer layers below the graphene, has a poisoning action. Rotated G domains, possibly forming above

nickel carbide, are more weakly adhered to the underlying substrate and thus are nearly inert.[27] These results are relevant for the atomistic understanding of the role of the substrate in determining the chemical reactivity of single layer graphene.

SUPPLEMENTARY MATERIAL

See supplementary material for a qualitative comparison of XPS spectra and for STM images of graphene films after CO dose.

ACKNOWLEDGMENTS

We acknowledge S. Agnoli (Università di Padova) for providing the G/Cu sample.

This work was funded by MIUR within the PRIN Project No. GRAF 20105ZZTSE_003, by the FIRB Futuro in Ricerca 2012 Project No. RBFR128BEC_004, and by PRA 2013.

[1] V. Georgakilas, M. Otyepka, A. B. Bourlinos, V. Chandra, N. Kim, K. C. Kemp, P. Hobza, R. Zboril, and K. S. Kim, Chem. Rev. **112**, 6156–6214 (2012).
[2] Q. Wu, Y. Wu, Y. Hao, J. Geng, M. Charlton, S. Chen, Y. Ren, H. Ji, H. Li, D. W. Boukhvalov, R. D. Piner, C. W. Bielawski, and R. S. Ruoff, Chem. Commun. **49**, 677–679 (2013).
[3] C. Morchutt, J. Bjork, S. Krotzky, R. Gutzler, and K. Kern, Chem. Commun. **51**, 2440–2443 (2015).
[4] Q. H. Wang, Z. Jin, K. K. Kim, A. J. Hilmer, G. L. C. Paulus, C.-J. Shih, M.-H. Ham, J. D. Sanchez-Yamagishi, K. Watanabe, T. Taniguchi, J. Kong, P. Jarillo-Herrero, and M. S. Strano, Nat. Chem. **4**, 724–732 (2012).
[5] A. Criado, M. Melchionna, S. Marchesan, and M. Prato, Angew. Chem., Int. Ed. **54**, 10734–10750 (2015).
[6] P. Lazar, F. Karlický, P. Jurečka, M. Kocman, E. Otyepková, K. Šafářová, and M. Otyepka, J. Am. Chem. Soc. **135**, 6372–6377 (2013).
[7] S. Schumacher, T. O. Wehling, P. Lazić, S. Runte, D. F. Förster, C. Busse, M. Petrović, M. Kralj, S. Blügel, N. Atodiresei, V. Caciuc, and T. Michely, Nano Lett. **13**, 5013–5019 (2013).
[8] F. Huttmann, A. J. Martínez-Galera, V. Caciuc, N. Atodiresei, S. Schumacher, S. Standop, I. Hamada, T. O. Wehling, S. Blügel, and T. Michely, Phys. Rev. Lett. **115**, 236101 (2015).
[9] M. Smerieri, E. Celasco, G. Carraro, A. Lusuan, J. Pal, G. Bracco, M. Rocca, L. Savio, and L. Vattuone, ChemCatChem **7**, 2328–2331 (2015).
[10] A. Garcia-Lekue, M. Ollé, D. Sanchez-Portal, J. J. Palacios, A. Mugarza, G. Ceballos, and P. Gambardella, J. Phys. Chem. C **119**, 4072–4078 (2015).
[11] E. Celasco, G. Carraro, A. Lusuan, M. Smerieri, J. Pal, M. Rocca, L. Savio, and L. Vattuone, Phys. Chem. Chem. Phys. **18**, 18692–18696 (2016).
[12] A. Ambrosetti and P. L. Silvestrelli, J. Chem. Phys. **144**, 111101 (2016).
[13] W. Zhao, S. M. Kozlov, H. Oliver, K. Gotterbarm, M. P. A. Lorenz, F. Viñes, C. Papp, G. Andreas, and H.-P. Steinrück, J. Phys. Chem. Lett. **2**, 759–764 (2011).
[14] W. Zhao, J. Gebhardt, K. Gotterbarm, O. Höfert, C. Gleichweit, C. Papp, A. Görling, and H.-P. Steinrück, J. Phys.: Condens. Matter **25**, 445002 (2013).
[15] L. L. Patera, C. Africh, R. S. Weatherup, R. Blume, S. Bhardwaj, C. Castellarin-cudia, A. Knop-gericke, R. Schloegl, G. Comelli, S. Hofmann, and C. Cepek, ACS Nano **7**, 7901–7912 (2013).
[16] C. T. Campbell, Surf. Sci. Rep. **27**, 1–111 (1997).
[17] M. C. Biesinger, B. P. Payne, L. W. M. Lau, A. Gerson, and R. S. C. Smart, Surf. Interface Anal. **41**, 324–332 (2009).
[18] R. S. Weatherup, B. C. Bayer, R. Blume, C. Baehtz, P. R. Kidambi, M. Fouquet, C. T. Wirth, R. Schlögl, and S. Hofmann, ChemPhysChem **13**, 2544–2549 (2012).
[19] D. E. Parreiras, E. A. Soares, G. J. P. Abreu, T. E. P. Bueno, W. P. Fernandes, V. E. de Carvalho, S. S. Carara, H. Chacham, and R. Paniago, Phys. Rev. B **90**, 155454 (2014).
[20] R. S. Weatherup, H. Amara, R. Blume, B. Dlubak, B. C. Bayer, M. Diarra, M. Bahri, A. Cabrero-Vilatela, S. Caneva, P. R. Kidambi, M.-B. Martin, C. Deranlot, P. Seneor, R. Schloegl, F. Ducastelle, C. Bichara, and S. Hofmann, J. Am. Chem. Soc. **136**, 13698–13708 (2014).
[21] F. P. Netzer and T. E. Madey, J. Chem. Phys. **76**, 710–715 (1982).
[22] J. Lahiri and M. Batzill, Appl. Phys. Lett. **97**, 023102 (2010).
[23] G. Chiarello, A. Cupolillo, C. Giallombardo, R. G. Agostino, V. Formoso, D. Pacilè, L. Papagno, and E. Colavita, Surf. Sci. **536**, 33–44 (2003).
[24] F. Bianchini, L. L. Patera, M. Peressi, C. Africh, and G. Comelli, J. Phys. Chem. Lett. **5**, 467–473 (2014).
[25] M. Wei, Q. Fu, Y. Yang, W. Wei, E. Crumlin, H. Bluhm, and X. Bao, J. Phys. Chem. C **119**, 13590–13597 (2015).
[26] Y. Gamo, A. Nagashima, M. Wakabayashi, M. Terai, and C. Oshima, Hyomen Kagaku **17**, 745–749 (1996).
[27] A. Dahal and M. Batzill, Nanoscale **6**, 2548 (2014).